A Proposal for a Parameterized Circulating Vector Field Guidance for Fixed Wing Unmanned Aerial Vehicles

A thesis presented to

the faculty of

the Russ College of Engineering and Technology of Ohio University

In partial fulfillment

of the requirements for the degree

Master of Science

Garrett S. Clem

December 2017

This thesis titled

A Proposal for a Parameterized Circulating Vector Field Guidance for Fixed Wing Unmanned Aerial Vehicles

by

GARRETT S. CLEM

has been approved for

the Department of Mechanical Engineering

and the Russ College of Engineering and Technology by

Jay P. Wilhelm

Assistant Professor of Mechanical Engineering

Dennis Irwin

Dean, Russ College of Engineering and Technology

Abstract

CLEM, GARRETT S., M.S., December 2017, Mechanical Engineering

A Proposal for a Parameterized Circulating Vector Field Guidance for Fixed Wing Unmanned Aerial Vehicles (32 pp.)

Director of Thesis: Jay P. Wilhelm

ABSTRACT

DED

ACKNOWLEDGMENTS

ACK

Table of Contents

Page

List of Tables

List of Figures

LIST OF SYMBOLS

a	Previous or Initial Axial Induction Factor (-)

List of Acronyms

AoA Angle of Attack

1 INTRODUCTION

1.1 Motivation and Problem Statement

Fixed wing Unmanned Aerial Vehicles are used for missions such as surveillance and reconnaissance that might put pilots harms way [1]. UAVs carry out mission objectives such as waypoint navigation and loitering by following paths that are typically pre-planned [2]. Known obstacles are avoided during the planning processes to avoid collisions. Paths must be of obstacles which may not be known during planning. Obstacles are not always known during planning and once discovered a new path may have to be re-planned. Guidance that follows mission paths while avoiding obstacles without the need for re-planning may be beneficial. Gradient vector field (GVF) guidance is a path following method that provides continuous guidance that guaranteed to converge and follow an arbitrary path. Guidance for getting on and following a path is produced by summing together convergence and circulation terms that are weighted by static scalars. Obstacles have been represented as separate repulsive GVFs that are later summed to the path following GVF [Wilhelm, Wambold, Clem]. Static GVFs do not always route the UAV around an obstacle and could be improved. Modifying the GVF convergence and circulation weights to be functions of common UAV states could be used to produce an optimal guidance for obstacle avoidance. **The proposed research seeks to determine GVF weighting functions that construct optimal obstacle avoidance.**

1.2 Methods Overview

The proposed research will be conducted in three phases where VF guidance singularities will be demonstrated, weighting functions will be investigated, and a developed GVF will be validated on a ground robot simulating a UAV. Phases I and II will be conducted in a simulation environment that combines mission paths and obstacles into a single GVF. Phase III will be conducted with a ground robot simulating a UAV guided by the modified GVF in real-time. Dubins fixed wing constraints will be imposed in simulations and experiments.

1.3 Phase I

Recreate gradient vector fields for circular and elliptical obstacles and demonstrate singularities. A simulation environment will be built that generates GVFs consisting of mission paths and obstacles. Circular and elliptical obstacles will be investigated and the resulting singularities will be characterized. Static weights will be used and the performance of the guidance measured in distance traveled and time of flight.

1.4 Phase II

Investigate GVF weighting functions that influence obstacle avoidance. UAV closing rate, position, and range will be used to develop dynamic GVF weights for convergence and circulation. The modified GVF will be compared against a static and strictly repulsive GVF. Distance traveled and time of flight will be used to as metrics to compare the modified GVF to the unmodified GVF.

1.5 Phase III

Validate modified GVF model with ground robot experiments. The modified GVF developed in Phase II will be implemented on a differential drive ground robot simulating a fixed wing UAV. Guidance performance while avoiding static obstacles will be demonstrated.

1.6 Summary of Phases

Each phase consists of an **objective** that will be accomplished by executing *tasks*. Completion of all objectives and phases will result in the final deliverable.

Phase I: Demonstrate Gradient Vector Field Singularities

1. *Build a GVF simulation environment*
2. *Derive GVF for circular and elliptical obstacles*
3. *Identify path and obstacles where singularities are produced*

Phase II: Investigate GVF weighting functions that influence obstacle avoidance

1. *Formulate circulation and convergence weights as functions of UAV state*
2. *Determine combination of GVF weights that produces optimal guidance in simulation*

Phase III: Validate modified GVF model with ground robot experiments

1. *Build differential drive robot*
2. *Build robotic framework to take guidance commands*
3. *Repeat simulations performed in Phase II on ground robot*

Deliverable: Adaptive GVF parameterized weights optimal guidance for path following and static obstacle avoidance.

2 Literature Review

2.1 Introduction to Literature Review

2.2 Unmanned Aerial Vehicle

Unmanned Aerial Vehicles (UAVs) are pilotless aircraft used by military, police, and civilian communities for tasks such as surveillance, reconnaissance, damage assessment, and natural disaster surveying. UAVs are generally categorized into fixed wing and rotor craft varieties that range in size, payload, and flight time capabilities. The aircrafts can be controlled remotely with a RC transmitter or fly on pre-planned paths executing maneuvers such as waypoint navigation and loitering. Data can be collected with on-board sensors such as cameras which then can be stored or relayed to the ground. UAVs are part of an Unmanned Aerial System (UAS) which is made up of the vehicle, autopilot, ground station, transmitter, and two way radio which is depicted in Figure 2.1. Ground stations are responsible for monitoring the vehicle's status, planning missions, and generating obstacle free and flyable paths which are sent to the autopilot via two way radio.

Figure 2.1: Unmanned Aerial System (UAS)

The autopilot is responsible for following the pre-planned path and maintaining vehicle stability while under the influence of external wind disturbances. Stable flight while path following is accomplished by implementing feed-back control, navigation, and guidance systems. Feed-back refers to the closure of an open-loop control system which allows an error to be calculated between the desired state of the UAV, the reference, and the current state of the UAV. Reference error is used to calculate the necessary actuator output required to modify the vehicles attitude and position while preventing unbounded osculations. Feed-back is provided by the navigation system which uses sensors to measure the attitude and position of the aircraft. Sensors often provide noisy data and are sampled at varying rates. Filtering and estimation techniques such as the Kalman filter which fuses and filters measurements to provide an improved state estimation. A high level overview of the autopilots systems can be seen in Figure 2.2.

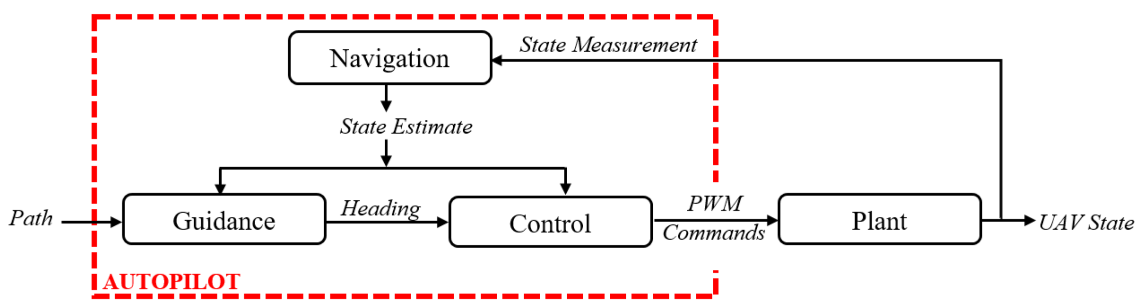

Figure 2.2: Autopilot's Navigation, Guidance, and Control Architecture

The navigation system is responsible for taking high level pre-planned paths from the ground station and providing a reference heading command to the control system. Several methods for path following guidance were investigated in [2] consisting of carrot chasing, non-linear guidance law, pure line-of-sight, linear quadratic regulator, and gradient vector field method. A Monte Carlo simulation with wind disturbances was conducted for the guidance methods above in [2]. It was determined that the vector field method followed the path with least tracking error and control effort which is the primary goal of path following.

2.3 Vector Field Guidance

2.3.1 Introduction to Vector Field Guidance

Vector field is a continuous guidance and control method that applies artificial attractive and repulsive forces to a point mass. The two broad categories of algorithms that produce vector fields consist of potential field algorithms and path following algorithms. Potential field produces guidance and control to a robot for converging to a distinct point. Path following algorithms produce guidance for converging and following a path. Several path following vector field algorithms have been investigated including gradient vector field, which provides convenient convergence and circulation weights that may be useful for providing an optimal guidance for obstacle avoidance.

2.3.2 Potential Field

Potential field was introduced as a real-time robotic manipulator algorithm for obstacle avoidance [4]. The potential field algorithm represents a robots workspace as a gradient potential of attractive and repulsive artificial forces that drive the robot to a desired goal. Goals are given the lowest potential and act as attractive forces. Obstacles have high potential and act as repulsive forces. A simple example is depicted in Figure 2.3 consisting of an initial state, a goal, and a single obstacle. The initial state of the robot is at the edge of a gradient where the potential is maximum. In the lowest part of the gradient a goal exists at the global minimum. Obstacles are added to the potential field, but have limited effect due to a decay function.

Potential field is unique in that path planning, trajectory planning, and control are lumped into a single system [6]. Transition from an initial state to a goal state traditionally

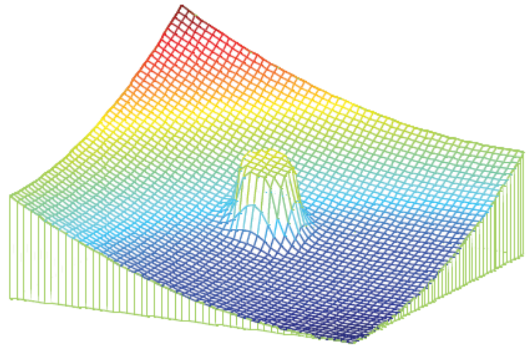

Figure 2.3: Single Obstacle Potential Field Gradient [5]

occurred by executing three steps consisting of path planning, trajectory planning, and control. Path planning dealt with finding an obstacle free path from an initial state to a goal state. Trajectory planning time parametrized the obstacle free path with some high level vehicle constraints considered. Lastly, control attempts to reduce the tracking error with respect to the reference trajectory. Combining the three motion planning steps into a single algorithm has been shown to be computational inexpensive [7].

As pointed out in [8], robots using potential field are susceptible to local minimum. Encountering a local minimum prevents the robot from continuing down the gradient and into the global minimum because equilibrium has been reached prematurely. Figure 2.4 demonstrates local minimum by adding several obstacles into a goal field. Several methods have been developed to mitigate the effects of local minimums as pointed out in [7] through the use of navigation functions. Local minimum produced as a result of closely spaced obstacles as shown in Figure 2.4 have been addressed by grouping obstacles together into a cluster [5].

Several methods have been developed to mitigate the effects of local minimums as pointed out in [7] through the use of navigation functions. Local minimum produced as a result of closely spaced obstacles as shown in Figure 2.4 have been addressed by grouping obstacles together into a cluster [5]. Grouping obstacles addresses the risk of

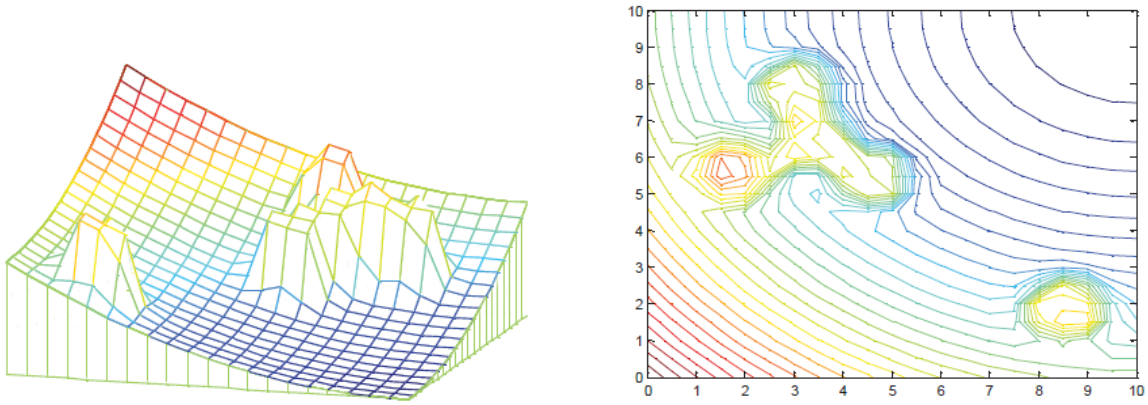

(a) (b)

Figure 2.4: Potential Field Local Minimum [5]

local minima before forming the potential field. If local minima are encountered after the field is generated, additional forces can be applied to push the robot away from the local minima.

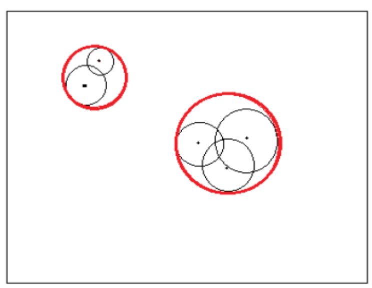

Figure 2.5: Obstacle Clustering [5]

Potential fields ability to avoid obstacles and combine path planning, trajectory planning, and control into a single system while being computationally inexpensive makes it an attractive option for many robotic systems. Fixed wing UAVs must maintain a minimum forward velocity and cannot converge to a single point, making potential field difficult to implement.

2.3.3 Virtual Force Field - Histogram Method

When the environment changes, such as a new obstacle or the goal has moved, the potential field has to be recalculated. Koren and Borenstein developed a virtual force field (VFF) histogram method that guides a mobile robot to a known goal while avoiding initially unknown obstacles [8]. VFF decomposes a robots workspace into discretized cells that contain an integer certainty value associated with the confidence that an obstacle occupies the cell. A global goal applies an artificial attractive force on the robot that pulls it closer to the goal. As the robot detects obstacles, the certainty value increases in the cell associated with the obstacles position. Cells apply artificial repulsive forces with magnitudes that depend on the certainty value and the distance to the cell.

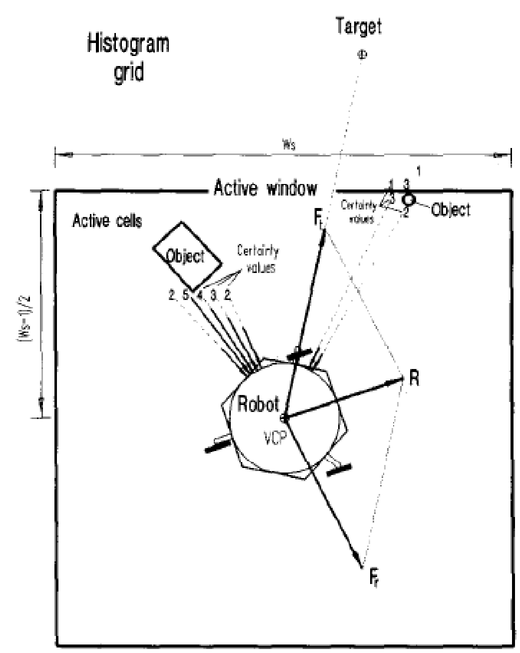

Figure 2.6: Virtual force field histogram acting on a mobile robot

The VFF histogram method was validated on a mobile robot platform using ultrasonic sensors in [8] and [9], avoiding obstacles and seeking a goal. Certainty cells in VFF only provide strictly repulsive vectors which guide the robot away, but provide no guidance for getting around the obstacle.

2.3.4 Lyapunov Vector Fields

Fixed wing UAVs must maintain a minimum forward velocity therefore cannot converge to a single point making potential field or VFF guidance difficult. Missions for UAVs are typically constructed from obstacle free paths build from straight line and circular arc primitives. Path planning provides a reference to the autopilot that guides the UAV to first arrive at and subsequently follow the desired path while under the influence of external disturbances. Ariving at and following the path are typically is typically achieved by generating vectors normal and parallel to the path respectively. Nelson et al. introduced a vector field generation method for straight line and circular arcs using Lyapunov stability arguments [10] and is depicted in Figure 2.7.

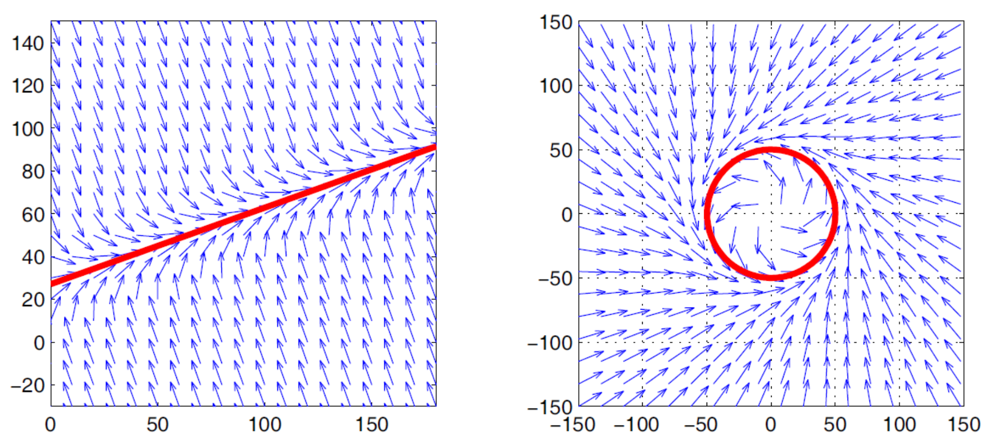

Figure 2.7: Lyapunov vector field for straight line and circular primitives

To construct flyable paths out of the primitives, it was necessary to determine how the resulting vector fields should be combined. Summing the fields directly result in dead-zones, sinks, and singularities. The solution was to have a single field active at any time, switching when the UAV reached the end of a primitive. Nelson's method was extended by Griffiths for curved path following and showed that the vectors asymptotically approach the curved path, shown in Figure 2.8.

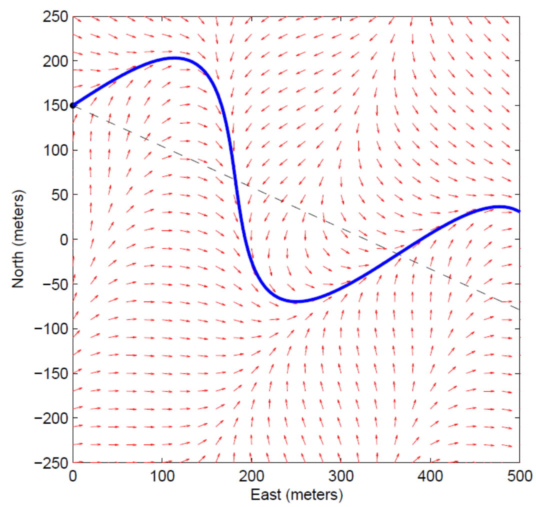

Figure 2.8: Lyapunov vector field approach curved path asymptotically

Primitive circular fields can be modified via non-linear coordinate transformations to produce globally convergent elliptical fields [11] [12]. Frew simulated and experimentally validated the transformed vector field where multiple fixed wing UAVs cooperatively tracked a moving target while maintaining a staggered distance from each other, preventing collision and multiple surveillance angles. The location of a target being tracked is not known with absolute certainty. The covariance matrix from a kalman filter to transform a circular vector field around an uncertain target was investigated in [12] and an example field is shown in Figure 2.9b.

A target tracking lyapunov plus tangent vector field was introduced in [13] that produced shorter paths compared to lyapunov alone. Outside of the standoff circle, tangent vectors were said to provide the shortest distance to the circle. Inside the standoff circle, no tangent lines exist and lyapunov is used in its place. Figure 2.10 shows the difference in

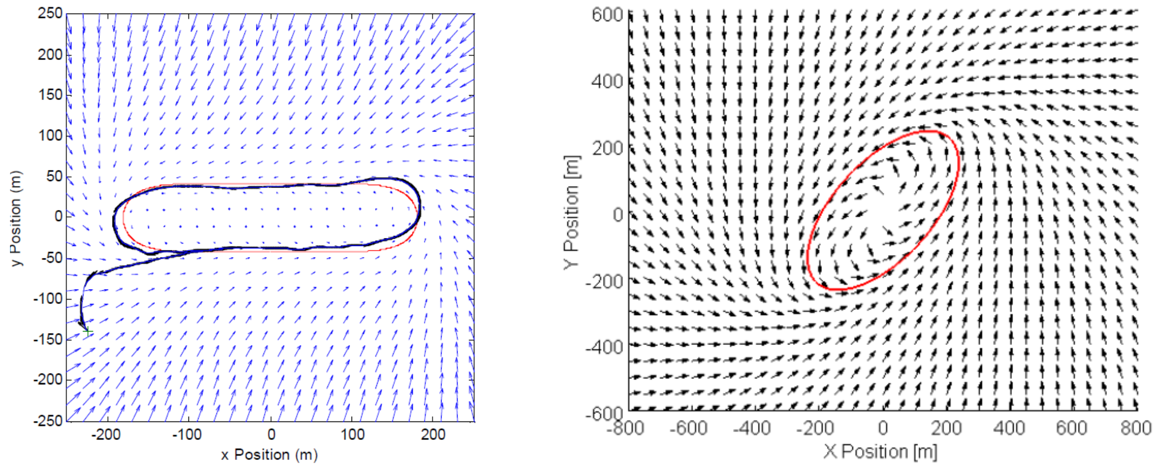

(a) (b)

Figure 2.9: Elliptical VF produced by non-linear coordinate transformations a) [11] b) [12]

paths taken for lyapunov and tangent vector fields outside the standoff circle. The TPLVF was later used for path planning to avoid obstacles in [14].

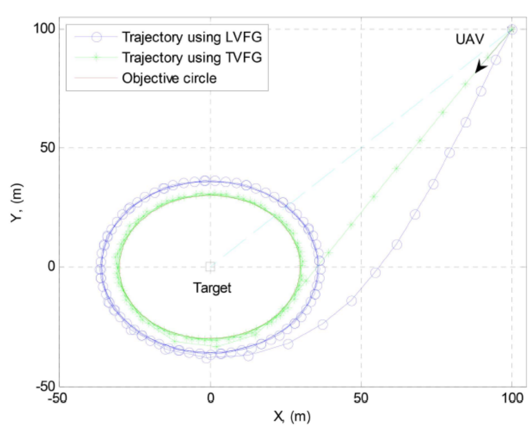

Figure 2.10: Tangent plus lyapunov vector fields for shortest path target tracking [14]

2.3.5 Non-Lyapunov Vector Fields

All methods that consider obstacles so far build a vector field that guides the UAV to an obstacle free path. Another approach is to build a vector field tending to a path and use optimal rapid random trees (RRT*) to explore the space for obstacles and select the optimal path. Pereia et al. developed such a method that builds a tree that makes up possible paths for the UAV to take. Branches extend from the root, or initial location of the UAV, randomly throughout the map with a constrained deviation from the initial vector field. When a branch encounters an obstacle it is trimmed and no longer explored. The path of minimum cost, or least distance, is selected for the UAV to use as a reference path. An example of the algorithm is shown in Figure 2.11.

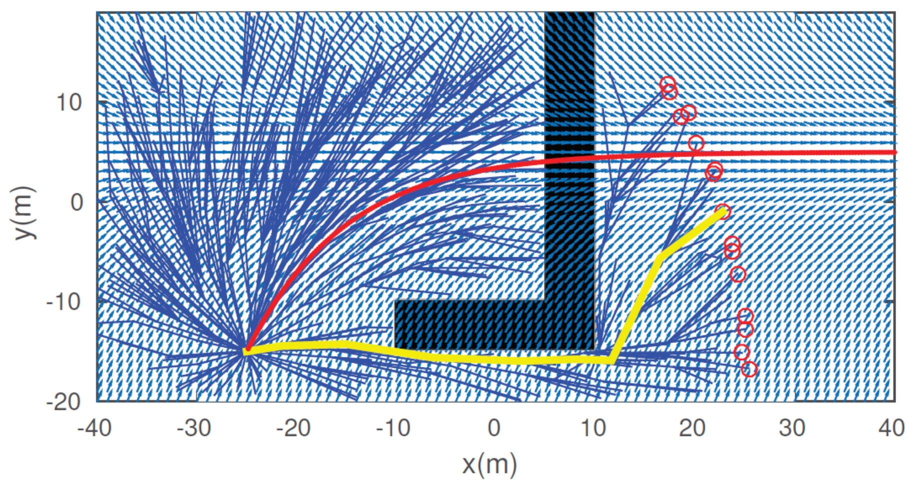

Figure 2.11: RRT* path planner with a VF used as a task specification

For well known obstacles in urban environments, such as buildings, an optimal path can be constructed with constrained delaunay triangulation (CDT) which has been previously used in computer animation [15]. CTD was used to construct vector fields in [16] that restricts robots movements inside the triangles while moving towards a global goal. A simulation of a robot traversing a vector field inside a set of CDTs can be seen in Figure 2.12.

So far all of the vector field methods discussed have avoided obstacles by planning paths around them. Paths are typically calculated at the ground station and if

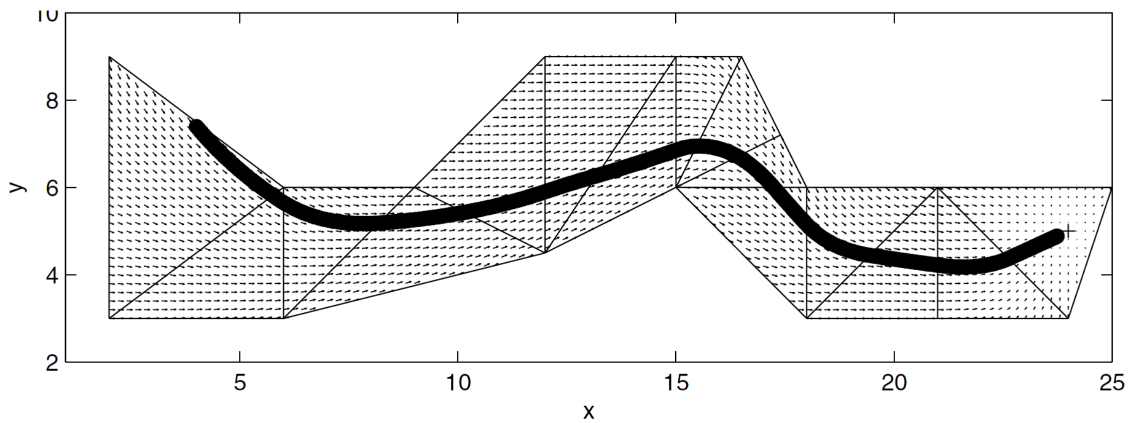

Figure 2.12: Vector field within a set of constrained delaunay triangles [16]

communication is lost a new path may not be relayed to a UAV encountering a new obstacle. A possible solution is using vector fields to provide a repulsive force, not unlike the VFF method, immigrating around the obstacle.

2.3.6 Gradient Vector Field

The gradient vector field method was first introduced in [17] and produces an n-dimensional vector field guaranteed to converge to a path made of points that lie at the intersection of two surfaces. The total vector field $\vec{V}$ is produced by summing together a convergence, circulation, and time varying terms seen in Equation **??**. Convergence terms contribute vectors normal to the path, circulation terms contribute vectors parallel to the path, and time varying vectors account for changes in the path as a function of time.

$$\vec{V} = \boldsymbol{G}\vec{V}_{conv} + \boldsymbol{H}\vec{V}_{circ} + \boldsymbol{L}\vec{V}_{tv} \tag{2.1}$$

Each term is multiplied by a scalar, $\boldsymbol{G}$, $\boldsymbol{H}$, $\boldsymbol{L}$, that weights the contribution of each term on the total field $\vec{V}$. Only static paths will be discussed so it is assumed the time varying field is null. The advantage of GVF is the convenient access to the weighting terms that independently effect the total field. Magnitude of the weights modifies the strength of each fields influence, whereas the sign indicates the direction. Figure 2.13 shows convergence and circulation fields for a circular path where the weights $\boldsymbol{G}$ and $\boldsymbol{H}$ are unity and positive. The convergence field contains vectors that are normal to the circular path for all points in space, with exception to the center of the circle which is undefined. Circulation fields contain vectors that are parallel to the path for all points in space with the same exception of no definition at the center of the circle.

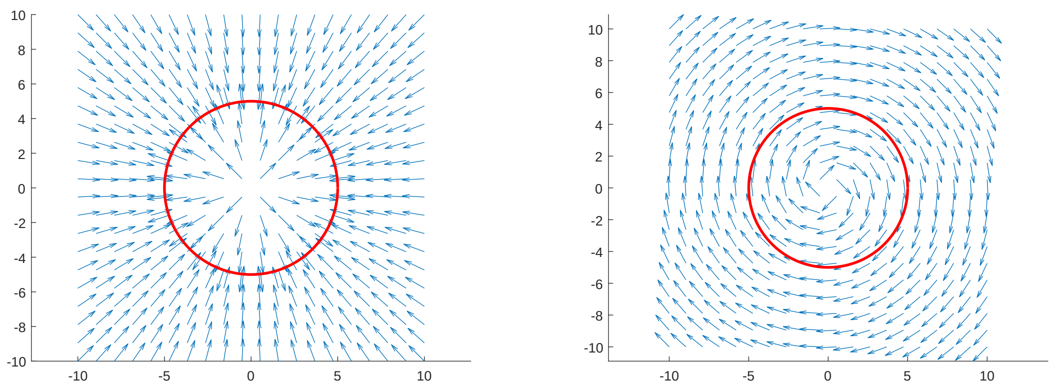

(a) (b)

Figure 2.13: Attractive vector field (a) and clockwise circulation field (b)

Modifying the signs of $\boldsymbol{G}$ and $\boldsymbol{H}$ to be unity and negative results in similar fields but with a 180° rotation about the center of the circle, Figure 2.14. The attractive convergence field becomes a repulsive field, where all vectors are anti-normal to the path. The circulation field changes direction and rotates counterclockwise around the path.

Repulsive fields have been used for obstacle avoidance for a UAV loitering around a moving target in [w,w,c]. A circular goal path was attached to a ground vehicle and a convergence and circulation vector field was generated. Circular paths were with small radii were placed on top of obstacles with strictly repulsive weights. Notice in Figure 2.14a that inside of the path, vectors guide inward, which is not desired for obstacle avoidance.

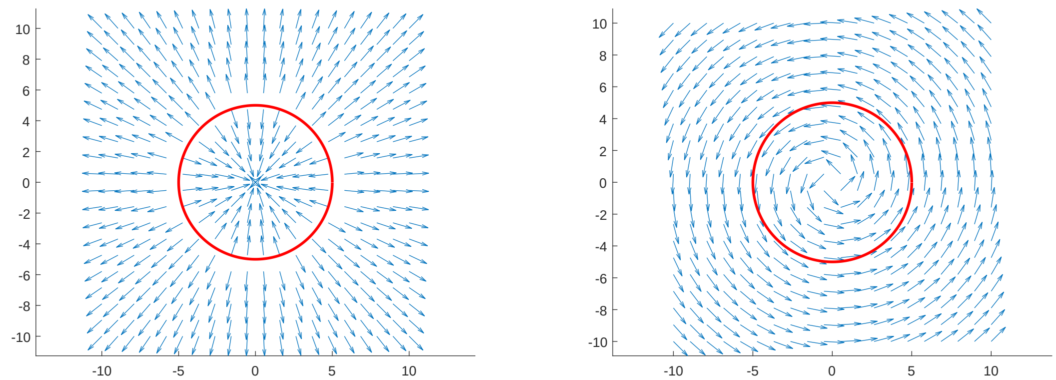

(a) (b)

Figure 2.14: Repulsive vector field a) and counterclockwise circulation field b)

The problem is aleviated by reducing the radius significantly. Goal and obstacle field are summed together to provide a total field that provides guidance to a UAV. Loitering is accomplished while avoiding two obstacles, as shown in Figure 2.15

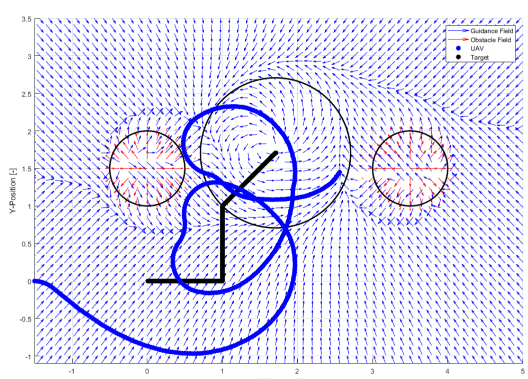

Figure 2.15: Place holder image of UAV following ground target

Similar to potential field and VFF, the strength of the repulsive field depends on the distance from an obstacle. In [w,w,c], a tangent hyperbolic decay function was assigned to the obstacle fields which varied the total strength from null to unity, shown in Figure 2.16.

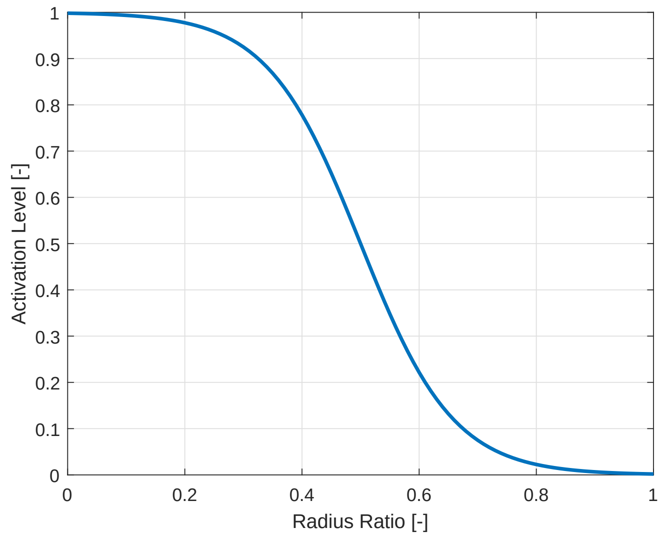

Figure 2.16:

Constructing the paths for a UAV flying at constant altitude requires three-dimensional surfaces intersecting to form two-dimensional paths. Consider a UAV in 2-dimensional space tracking a path τ, which is made of points that lie at the intersection of two surfaces. Each of the surfaces α_i is continuous, differentiable, and is a function of the set $q = [x, y, z]$. The convergence field $\vec{V_{conv}}$ is produced by the sum of surfaces multiplied by their respective partial gradient $\nabla_q \alpha_i$. The definition of the convergence field is summarized in Equations 2.2 and 2.3.

$$\vec{V}_{conv} = \boldsymbol{G} \sum_{i=1}^{n-1} \alpha_i \nabla_q \alpha_i \tag{2.2}$$

$$\nabla_q = \begin{bmatrix} \frac{\partial}{\partial x} \\ \frac{\partial}{\partial y} \\ \frac{\partial}{\partial z} \end{bmatrix} \tag{2.3}$$

To produce a circular path of radius r the intersection of a cylinder and plane are used, as shown in Equations 2.4-2.5 and pictured in Figure 2.17.

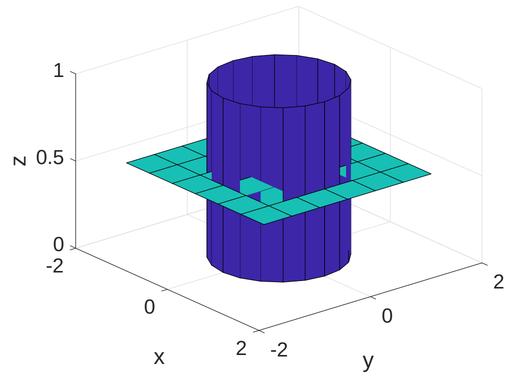

Figure 2.17:

$$\alpha_1 = x^2 + y^2 - r \tag{2.4}$$

$$\alpha_2 = z \tag{2.5}$$

Convergence vector field term is produced by taking the wedge product of the partials $\nabla_q \alpha_i$, which in three dimensions simplifies to the cross product as shown in Equations 2.6 and 2.7.

$$\vec{V}_{circ} = \boldsymbol{H} \wedge_{i=1}^{n-1} \nabla_q \alpha_i \tag{2.6}$$

$$\vec{V}_{circ} = \boldsymbol{H}(\nabla_q \alpha_1 \times \nabla_q \alpha_2) \tag{2.7}$$

Circulation and convergence terms may have different magnitudes depending on the location of origin of a vector and the equations used for surfaces. Normalizing each component prior to weighting allows for more predictable results when assigning values. So far the VF weights have been used for high level specification of the desired behavior for a UAV, whether it be for convergence, avoidance, or circulation. Furthermore, there is no guarauntee that when using a vector field for avoidance that the UAV will not violate the no-fly zone. If the UAV turn rate is at saturation an increased reference command will do nothing to aid in avoidance. A demonstration of saturation is seen in Figure 2.18 where a UAV is provided guidance by a convergent and circulating vector field about a circular path.

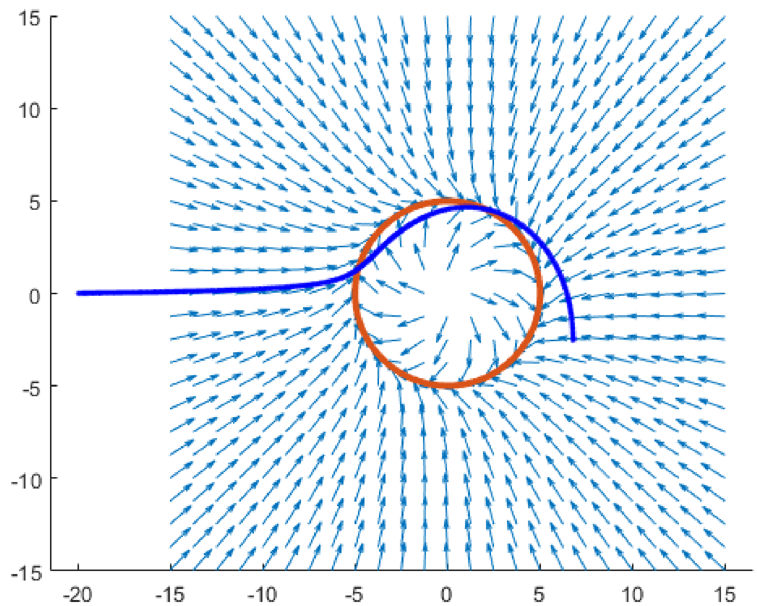

Figure 2.18: Dubins UAV actuator saturation

If the VF was adjusted earlier at an earlier state, the tracking error may be reduced. When using an obstacle, determining which direction the UAV must fly around the obstacle is important to reduce distance flown. Determining functions for the sign and magnitude of the vector field weights to produce an optimal guidance.

2.4 Unmanned Aerial Vehicle Simulation

Testing new guidance, navigation, and control algorithms can be costly, require significant time, and requires an adequately large airspace. Ground stations need to be established which require power and shelter. Some small fixed wing UAVs may not be suitable to fly in all weather, therefore test flights may be canceled due to weather conditions. Lastly, larger UAVs need to have FAA clearance before flight which has to be pre-approved and takes time. Before spending the time to reserve airspace and allocate man hours for flight tests it is important to test algorithms in a controlled environment. One way to accomplish testing without actual flight is through validation through mobile robots simulating fixed wing constraints [18], [19], [20]. Programming a mobile robot, such as one shown in Figure

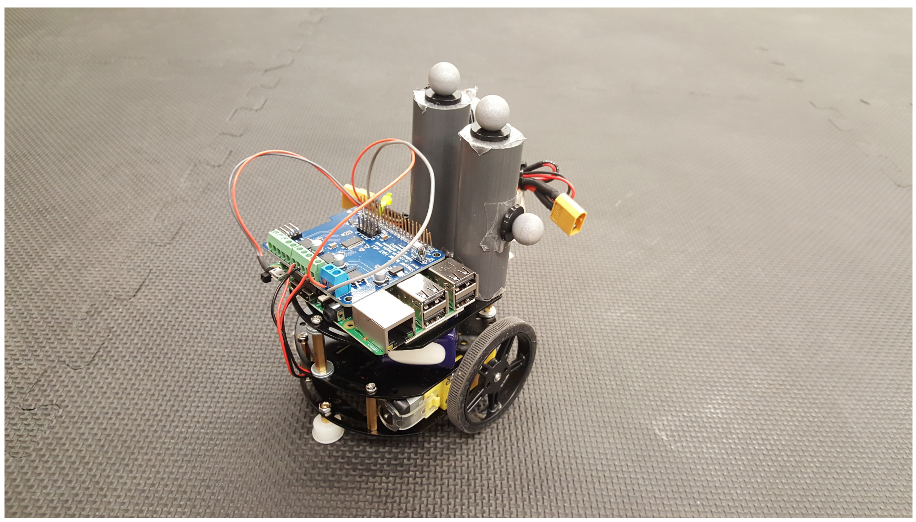

Figure 2.19: Differential drive mobile robot simulating fixed wing UAV Dubins constraints

2.5 Literature Review Summary

•

References

[1] Bone, E., "UAVs backbround and issues for congress.pdf," 2003.

[2] Sujit, P., Saripalli, S., and Sousa, J. B., "Unmanned Aerial Vehicle Path Following: A Survey and Analysis of Algorithms for Fixed-Wing Unmanned Aerial Vehicless," *IEEE Control Systems*, Vol. 34, No. 1, Feb. 2014, pp. 42–59.

[3] Beard, R. W. and McLain, T. W., *Small unmanned aircraft: theory and practice*, Princeton University Press, Princeton, N.J, 2012, OCLC: ocn724663112.

[4] Khatib, O., "Real-time obstacle avoidance for manipulators and mobile robots," *The international journal of robotics research*, Vol. 5, No. 1, 1986, pp. 90–98.

[5] Liu, Y. and Zhao, Y., "A virtual-waypoint based artificial potential field method for UAV path planning," *Guidance, Navigation and Control Conference (CGNCC), 2016 IEEE Chinese*, IEEE, 2016, pp. 949–953.

[6] Rimon, E., "Exact Robot Navigation Using Artificial Potential Functions.pdf," 1992.

[7] Goerzen, C., Kong, Z., and Mettler, B., "A Survey of Motion Planning Algorithms from the Perspective of Autonomous UAV Guidance," *Journal of Intelligent and Robotic Systems*, Vol. 57, No. 1-4, Jan. 2010, pp. 65–100.

[8] Borenstein, J. and Koren, Y., "Real-time obstacle avoidance for fast mobile robots in cluttered environments," *Robotics and Automation, 1990. Proceedings., 1990 IEEE International Conference on*, IEEE, 1990, pp. 572–577.

[9] Borenstein, J. and Koren, Y., "The vector field histogram-fast obstacle avoidance for mobile robots," *IEEE transactions on robotics and automation*, Vol. 7, No. 3, 1991, pp. 278–288.

[10] Nelson, D. R., "Cooperative control of miniature air vehicles," 2005.

[11] Frew, E., "Lyapunov Guidance Vector Fields for Unmanned Aircraft Applications.pdf," .

[12] Frew, E. W., "Cooperative standoff tracking of uncertain moving targets using active robot networks," *Robotics and Automation, 2007 IEEE International Conference on*, IEEE, 2007, pp. 3277–3282.

[13] Chen, H., Chang, K., and Agate, C. S., "Tracking with UAV using tangent-plus-Lyapunov vector field guidance," *Information Fusion, 2009. FUSION'09. 12th International Conference on*, IEEE, 2009, pp. 363–372.

[14] Chen, H., Chang, K., and Agate, C. S., "UAV path planning with tangent-plus-Lyapunov vector field guidance and obstacle avoidance," *IEEE Transactions on Aerospace and Electronic Systems*, Vol. 49, No. 2, 2013, pp. 840–856.

[15] Md, Z., Rg, C., and Dj, G., "Simplex Solutions for Optimal Control Flight Paths in Urban Environments," *Journal of Aeronautics & Aerospace Engineering*, Vol. 06, No. 03, 2017.

[16] Pimenta, L. C., Pereira, G. A., and Mesquita, R. C., "Fully continuous vector fields for mobile robot navigation on sequences of discrete triangular regions," *Robotics and Automation, 2007 IEEE International Conference on*, IEEE, 2007, pp. 1992–1997.

[17] Goncalves, V. M., Pimenta, L. C. A., Maia, C. A., and Pereira, G. A. S., "Artificial vector fields for robot convergence and circulation of time-varying curves in n-dimensional spaces," IEEE, 2009, pp. 2012–2017.

[18] Ren, W., McLain, T., Sun, J.-S., and Beard, R., "Experimental validation of an autonomous control system on a mobile robot platform," *IET Control Theory & Applications*, Vol. 1, No. 6, Nov. 2007, pp. 1621–1629.

[19] Louali, R., Djouadi, M. S., Nemra, A., Bouaziz, S., and Elouardi, A., "Designing embedded systems for fixed-wing UAVs: Dynamic models study for the choice of an emulation vehicle," IEEE, Feb. 2014, pp. 1–6.

[20] Louali, R., Elouardi, A., Bouaziz, S., and Djouadi, M. S., "Experimental Approach for Evaluating an UAV COTS-Based Embedded Sensors System," *Journal of Intelligent & Robotic Systems*, Vol. 83, No. 2, Aug. 2016, pp. 289–313.